Nanoparticles with antioxidant enzymes protect injured spinal cord from neuronal cell apoptosis by attenuating mitochondrial dysfunction

Syed Suhail Andrabi, Jun Yang, Yue Gao, Youzhi Kuang, Vinod Labhasetwar

PII: S0168-3659(19)30716-3

DOI: https://doi.org/10.1016/j.jconrel.2019.12.001

Reference: COREL 10044

To appear in: *Journal of Controlled Release*

Received date: 28 August 2019

Revised date: 26 November 2019

Accepted date: 1 December 2019

Please cite this article as: S.S. Andrabi, J. Yang, Y. Gao, et al., Nanoparticles with antioxidant enzymes protect injured spinal cord from neuronal cell apoptosis by attenuating mitochondrial dysfunction, *Journal of Controlled Release* (2019), https://doi.org/10.1016/j.jconrel.2019.12.001

Nanoparticles with antioxidant enzymes protect injured spinal cord from neuronal cell apoptosis by attenuating mitochondrial dysfunction

Syed Suhail Andrabi, Jun Yang[#], Yue Gao, Youzhi Kuang, Vinod Labhasetwar*

Department of Biomedical Engineering, Lerner Research Institute, Cleveland Clinic, Cleveland, OH, 44195, USA.

Running title: Protecting spinal cord from mitochondrial dysfunction and apoptosis

Key Words: Nanoparticles, Antioxidant Enzymes, Reactive Oxygen Species, Neurodegeneration, Biodegradable Polymer, Sustained Release

SSA, JY, and YG made an equal contribution to this study.

#Current affiliation: Department of Neurosurgery, Xiang'an Hospital of Xiamen University, School of Medicine, Xiamen University, Xiamen, China

***Author for correspondence:**
Vinod Labhasetwar, Ph.D.
Department of Biomedical Engineering/ND20
Cleveland Clinic
9500 Euclid Avenue
Cleveland, OH 44195
Tel: 216/445-9364; Fax: 216/444-9198
E-mail: labhasv@ccf.org

Abstract

In spinal cord injury (SCI), the initial damage leads to a rapidly escalating cascade of degenerative events, known as secondary injury. Loss of mitochondrial homeostasis after SCI, mediated primarily by oxidative stress, is considered to play a crucial role in the proliferation of secondary injury cascade. We hypothesized that effective exogenous delivery of antioxidant enzymes — superoxide dismutase (SOD) and catalase (CAT), encapsulated in biodegradable nanoparticles (nano-SOD/CAT) — at the lesion site would protect mitochondria from oxidative stress, and hence the spinal cord from secondary injury. Previously, in a rat contusion model of severe SCI, we demonstrated extravasation and retention of intravenously administered nanoparticles specifically at the lesion site. To test our hypothesis, a single dose of nano-SOD/CAT in saline was administered intravenously 6 hrs post-injury, and the spinal cords were analyzed one week post-treatment. Mitochondria isolated from the affected region of the spinal cord of nano-SOD/CAT treated animals demonstrated significantly reduced mitochondrial reactive oxygen species (ROS) activities, increased mitochondrial membrane potential, reduced calcium levels, and also higher adenosine triphosphate (ATP) production capacity than those isolated from the spinal cords of untreated control or SOD/CAT solution treated animals. Although the treatment did not achieve the same mitochondrial function as in the spinal cords of sham control animals, it significantly attenuated mitochondrial dysfunction following SCI. Further, immunohistochemical analyses of the spinal cords of treated animals showed significantly lower ROS, cleaved caspase-3, and cytochrome c activities, leading to reduced spinal cord neuronal cell apoptosis and smaller lesion area than in untreated animals. These results imply that the treatment significantly attenuated progression of secondary injury that is also reflected from less weight loss and improved locomotive recovery of treated vs. untreated animals. In conclusion, nano-SOD/CAT mitigated activation of cascade of degenerating factors by protecting mitochondria and hence the spinal cord from secondary injury. An effective treatment during the acute phase following SCI could potentially have a positive long-term impact on neurological and functional recovery.

Abbreviations

ATP:	Adenosine Triphosphate
BSA:	Bovine Serum Albumin
CAT:	Catalase
ETC:	Electron Transport Chain
IV:	Intravenously
MMP:	Mitochondrial Membrane Potential
NPs:	Nanoparticles
nano-SOD/CAT:	Nanoparticles encapsulating SOD and CAT
PLGA:	Poly (D,L-lactide *co*-glycolide)
PVA:	Poly (vinyl alcohol)
ROS:	Reactive Oxygen Species
SCI:	Spinal Cord Injury
SOD:	Superoxide dismutase
TEM:	Transmission Electron Microscopy

Introduction

Spinal cord injury (SCI) leads to initial damage followed by a rapidly escalating cascade of degenerative events, known as secondary injury [1]. With time, the secondary injury cascade aggravates the initial damage, resulting in increasing spinal cord neuronal cell death. A timely therapeutic intervention that inhibits the progression of secondary injury during the acute phase after the injury (2-48 hours) can have a significant impact on long-term neurological and functional recovery. Under normal conditions, mitochondria play a significant role in cellular bioenergetics, function, and survival; however, after SCI, the lack of adequate oxygen and glucose supply to the spinal cord due to ischemic condition causes mitochondria to undergo a series of biochemical changes [2]. These changes, such as mitochondrial membrane potential (MMP) and electron transport chain (ETC), disrupt the mitochondria's ability to produce adenosine triphosphate (ATP), the primary source of cellular energy [3]. As a result, there is a loss of ATP-dependent cellular functions, resulting in calcium overload and an increase in oxidative stress [4]. In addition to excessive production of reactive oxygen species (ROS), various apoptotic factors (e.g., caspase, cytochrome c) are activated, culminating in the initiation of degenerative cascade that eventually leads to more spinal cord neuronal cell death with time after the injury [5].

A therapeutic strategy aimed at mitigating mitochondrial dysfunction or restoring mitochondrial function during the acute phase of secondary injury could potentially inhibit the progressive degeneration of the injured spinal cord with time. SCI induces a detrimental self-proliferating cycle of increased ROS production, with mitochondria being the primary source of their formation, leading to oxidative damage to cell membrane, proteins, and DNA [6]. Under normal conditions, ROS are continuously produced by mitochondria as a part of normal cellular metabolic activity, but the endogenous antioxidant enzymes present in cells/tissue neutralize them. However, this redox balance is lost when excess ROS are formed under traumatic conditions such as after SCI. In addition, the genes for antioxidant enzymes are also downregulated after the injury, creating an oxidative stress condition [7]. Since ROS directly target the complexes in the mitochondrial respiratory chain [8], they play a critical role in mitochondrial dysfunction after SCI [9].

Neutralizing excess ROS formed after SCI with exogenously delivered antioxidant enzymes to regain the redox balance could potentially stabilize mitochondria under stress, thus inhibiting the propagation of secondary injury cascades. In this study, we explored the efficacy of a combination of antioxidant enzymes, superoxide dismutase (SOD) and catalase (CAT), encapsulated in sustained release biodegradable nanoparticles (NPs) (nano-SOD/CAT). Dismutation of superoxide radicals with SOD leads to the formation of hydrogen peroxide, a toxic molecule, which is neutralized by CAT to form inert, water and oxygen molecules [10]; hence, the combination of two enzymes was used in nano-SOD/CAT formulation. Contusion injury results in breakdown of the blood-spinal cord barrier at the impacted site [11]; hence, intravenously administered NPs from systemic circulation can specifically extravasate to the lesion site. Also, the injury triggers an inflammatory response that can further make the vasculature leaky at the lesion site for NPs to extravasate at the lesion site [12]. In our recent study, we demonstrated dose-dependent localization of intravenously administered NPs, more specifically at the lesion site than in other uninjured segements of the spinal cord. Further, the NPs localized at the lesion site were shown to be retained for a prolonged period (>1 wk) [13]. In

this study, we hypothesized that localization and sustained retention of nano-SOD/CAT at the lesion site following intravenous administration would mitigate the oxidative stress condition, thus attenuating the post-injury mitochondrial dysfunction, thus protecting the spinal cord from further neuronal cell apoptosis and degeneration. We tested our hypothesis in a rat contusion model of severe SCI. Nano-SOD/CAT was administered intravenously 6 hrs post-injury, and the spinal cords were analyzed at 1-wk post-treatment.

Materials and Methods

Materials: Poly (D,L-lactide *co*-glycolide) (PLGA; 50:50, inherent viscosity of 0.76-0.94 dL/g) was purchased from LACTEL Absorbable Polymers (Birmingham, AL). Poly (vinyl alcohol) (PVA; 87-90% hydrolyzed, mol. wt. 30,000-70,000), Bovine Serum Albumin (BSA), Superoxide Dismutase (SOD) from bovine red blood cells with activity of ~3,000 units/mg, Catalase (CAT) from bovine liver with activity of 2,000-5,000 units/mg, Dimethyl tartaric acid (DMT), Tween-80 glucose and Triton X-100 were purchased from Sigma-Aldrich (St. Louis, MO). Chloroform of HPLC grade was obtained from Fisher Scientific (Pittsburgh, PA).

Analysis of SOD and CAT activities: Prior to their use in formulating nano-SOD/CAT, SOD and CAT activities were determined using the SOD (Dojindo Molecular Technologies, Inc. Rockville, MD, Catalog number, S311-10) and CAT (Sigma Aldrich, Catalog Number CAT100) Assay Kits.

Formulation of nano-SOD/CAT: To formulate nano-SOD/CAT, SOD- and CAT-loaded NPs (nano-SOD, nano-CAT) were prepared separately and mixed in 1: 2 w/w ratio during the last processing step as described below. These were formulated by a double water-in-oil-in-water (w/o/w) emulsion solvent-evaporation method. In a typical preparation, 1X batch of nano-SOD and 2X batch of nano-CAT (i.e., 1: 2 w/w ratio of nano-SOD and nano-CAT) were prepared simultaneously. To prepare 1X batch of nano-SOD, 12 mg SOD and 18 mg BSA were dissolved in 300 µL MQ water. To prepare 2X batch of nano-CAT, 16 mg CAT and 44 mg BSA were dissolved in 600 µL Milli-Q water. The enzyme solution prepared as above was emulsified into a polymer solution containing 162 mg PLGA (with 18 mg DMT) in 6 mL chloroform. The primary w/o emulsion was formed, first by vortexing for 1 min, followed by sonication for 2 min on an ice bath using a stepped microtip probe at 40% power (Qsonica LLC, Model Q500, Newtown, CT).

For each 1X batch, the above w/o emulsion was emulsified into 18 mL of 3% w/v PVA solution in water, which is saturated with chloroform by adding 50 µl chloroform in PVA solution, first by vortexing for 1 min, followed by sonication as above for 4 min to form multiple (w/o/w) emulsion. The emulsion was stirred overnight (~18 hrs) on a magnetic stir plate at 1,000 rpm in a fume hood at room temperature with an airflow set at a face velocity of 200 feet/min (6,400 cm/min). The formed NP dispersion was stirred for an additional one hour in a desiccator under vacuum (at ~ 23 psi) to ensure removal of chloroform.

At this stage, 1X batch of nano-SOD and 2X batch of nano-CAT formulated as above were mixed. The formulation of nano-SOD/CAT was recovered by ultracentrifugation at 30,000 rpm (82,000 x g) (Optima XE-90 with a 50.2Ti rotor, Beckman Coulter, Brea, CA) for 30 min. The supernatant was removed and the pellet was resuspended in autoclaved Milli-Q water (ASTM

Type 1 water, EMD Millipore Super-Q Plus filtration system; EMD Millipore, Darmstadt, Germany). The above process of centrifugation and resuspension of NPs was repeated two times to remove excess PVA, as well as the unencapsulated BSA and enzymes. The supernatant and washings were saved to analyze the amount of enzymes that are not encapsulated (see below).

After a final re-suspension and sonication of the pellet as above, it was centrifuged at 1,000 rpm (216 x g) for 10 min (Thermo Electron Sorvall Legend RT Plus, Thermo Scientific, Waltham, MA) to remove large aggregates, if any. The supernatant was collected, to which glucose was added as a cryoprotectant (2% w/v of NP suspension, the volume of NP suspension = 20 ml or ~1:4 w/w NPs to Glucose). Based on the doses of the formulation for each animal, appropriate aliquots of nano-SOD/CAT dispersion were made in pre-weighted cryovials (Nunc, Roskilde, Denmark) and then the samples in vials were frozen at -80 °C in a freezer and lyophilized using a Freezone 4.5 (Labconco, Kansas City, MO) for 2 days at 0.016 mBar and -55 °C. The added glucose before lyophilization helps in re-dispersing nano-SOD/CAT in saline with gentle mixing. To estimate the amount of nano-SOD/CAT in each vial, a few representative vials containing only added glucose were lyophilized and weighted. The average difference in the weight was used to calculate nano-SOD/CAT amount in each vial. The vials were stored at -20 °C until used for animal studies.

Characterization of nano-SOD/CAT: Hydrodynamic diameter and zeta potential of nano-SOD/CAT were determined using NICOMP 380 ZLS (Particle Sizing Systems, Port Richey, FL). A stock dispersion of lyophilized nano-SOD/CAT was prepared in MQ water (2 mg/ml). Three µl of the above stock was diluted to 0.5 ml in MQ water for measuring particle size and 100 µl of the stock was diluted to 3 ml in MQ water for measuring zeta potential. The size of NPs was measured at a scattering angle of 90º at 25 ºC. Zeta potential was measured in the phase-analysis mode and the current mode at a scattering angle of -14º. For transmission electron microscopy (TEM), a drop of dispersion of nano-SOD/CAT in water (~250 µg/mL) was placed on a 200 mesh Formvar-coated TEM grid with a size of 97 µm (TED PELLA, Redding, CA). The sample was negatively stained with 2% w/v uranyl acetate solution for a min, washed with sterile MiliQ water, and air dried for 3 h. The sample was imaged at 200 kV (Philips 201 TEM, Philips/FEI Inc., Brianchiff Manor, NY). The mean particle diameter was determined from different images using ImageJ software.

Encapsulation efficiency and *in vitro* release of SOD and CAT from nano-SOD/CAT: Since the formulation of nano-SOD/CAT contains both the enzymes, we first determined that there is no interference in activity of SOD to CAT and vice versa when both were assayed using the respective kits. To determine the encapsulation efficiency of each enzyme in nano-SOD/CAT, the supernatant and washings following their recovery using ultracentrifugation as described above under the formulation protocol were assayed for SOD and CAT activities. The encapsulation efficiency for each enzyme was determined from the difference in the amount of each enzyme added in the formulation and the amount that was seen in the supernatant and washings. We previously used such an indirect method to determine encapsulation efficiency, as direct extraction of enzymes/proteins from NPs using organic solvents such as methylene chloride or chloroform leads to their inactivation/denaturation and incomplete recovery [14].

To determine release of the encapsulated enzymes, lyophilized nano-SOD/CAT formulation (1 mg/ml, 2 ml) was dispersed in PBS buffer (150 mM, pH 7.4) containing BSA (0.1% w/v) and Tween-80 (0.05%) as stabilizing agents for enzymes [15]. Nano-SOD/CAT dispersion was prepared in 5 ml Eppendorf tubes by first vortexing the sample for 1 min followed by 10 min water-bath sonication (FS-30, Fisher Scientific). The tubes were incubated at 37 °C on a shaker rotating at 110 rpm (Environ, Lab-line Instruments, Barnstead International Inc, Dubuque, IA). At intervals of 1, 3, and 7 days post-incubation, 20 µl of sample was withdrawn, the samples were centrifuged at 2,000 rpm for 5 min (Thermo Electron Sorvall Legend RT Plus, Thermo Scientific, Waltham, MA) and supernatants were assayed for the SOD and catalase activities using the respective assay kits. From the total amount of enzymes released and encapsulation efficiency as determined above, cumulative percent release of each enzyme was determined.

Animal Studies

Rat model of SCI: The Cleveland Clinic's Institutional Animal Care and Use Committee approved the animal procedures, and these studies were carried out according to the Federal and internal guidelines. Sprague-Dawley rats (male/female) 6 to 8 weeks old were obtained from Envigo (Cleveland, OH). Animals were housed in a temperature- and light-controlled room on a 12-hr light, 12-hr dark cycle with free access to water and food. Following laminectomy, the spinal cord was exposed at T10. SCI was induced using Infinite Horizon (IH) impactor (Model IH-0400, Precision Systems and Instrumentation, LLC, VA) with an impact force of 250 Kdyn and a velocity of 10 mm/s with a dwelling time of 15 sec. As per the manufacturer, these conditions are set to induce a "severe" contusion SCI. Bladder expression was performed manually twice daily. Each animal weight was recorded pre- and post-injury at 1 wk and the difference in the weight was used to calculate weight loss in both treated and untreated control groups.

Administration of nano-SOD/CAT: Following SCI, a dose of 30 mg/kg nano-SOD/CAT in 0.8 ml normal saline (each mg of nano SOD/CAT contained 749.9 ± 5.6 units or ~133 µg of SOD and 814.6 ± 3.5 units or ~167 µg of CAT) or equivalent amount of SOD/CAT enzymes in saline (SOD= 3,990 µg/kg CAT= 5,023 µg/kg) was administered via tail vein at 6 hours post-injury; untreated control received saline only. In sham control animals, laminectomy was performed as above, but no injury was induced or any treatment was given. Animals were euthanized at 1 wk post-treatment.

BBB scoring: Animals were assessed for open field locomotion by one blinded observer using the Basso-Beattie-Bresnahan (BBB) locomotor rating scale [16] at 1 wk post-SCI. This 21-point scale represents several stages during recovery such as movement of joints, forelimb and hindlimb coordination, trunk stability, toe clearance and tail position. From 0 to 7 is related to movement of the joints and 8 to 21 are related to planter stepping and consistent coordination of gait.

Harvesting of spinal cord: Following euthanasia, blood was drained via cardiac puncture followed by perfusion of animals with normal saline. Laminectomy was performed to isolate spinal cords which were immediately placed in freshly prepared ice-cold mitochondrial isolation medium (225 mM sucrose, 75 mM mannitol, 1 mM EGTA ((ethylene glycol-bis (β-aminoethyl ether)-N,N,N′,N′-tetraacetic acid), 5 mM HEPES [4-(2-hydroxyethyl)-1-

piperazineethanesulfonic acid] buffer pH 7.4 in a glass petri dish. Spinal cords collected as above were used for isolating and characterization of mitochondria as described below. In the case of spinal cords that were used for immunohistochemical analysis, animals underwent trans-cardiac perfusion with normal saline as above, followed by perfusion with 4% paraformaldehyde in 1X PBS, pH 7.4 (PFA, Sigma).

Mitochondrial isolation: Mitochondrial isolation procedures were performed in ice-cold conditions, and were characterized within 5 hrs of their isolation. A two-cm segment of each spinal cord segment that included the lesion site was homogenized in 2 ml isolation medium by using Minilys homogenizer for 2 min (Bertin Technologies, Montigny-le-Bretonneux, France). The homogenate was centrifuged at 1,300 g at 4 °C for 8 min (Beckman Coulter, Lakeview Parkway, IN). The supernatant was transferred into a new 50 ml tarson tube (Polypropylene/Spinwin Conical-Bottom, BD Falcon, San Jose, CA) and centrifuged as above at 21,000 g at 4 °C for 10 min. The pellet was re-suspended in 3.5 ml of 15 % Percoll (P1644 Sigma-Aldrich); the suspension was layered slowly above the 24%-40% Percoll using a disposable pipette. The tubes were centrifuged at 30,700 g at 4 °C for 10 min. The layer that is enriched in mitochondria accumulates at the interface between the 40% and the 24%. Percoll was collected and resuspended in 2 ml of isolation medium without EGTA. The protein content of each sample was determined using a Bio-Rad protein assay kit (Cat#5000002, Alfred Nobel Drive Hercules, CA). The samples were adjusted to the same protein content prior to flow cytometric analysis, as described below.

Flow cytometric analysis for mitochondrial membrane potential, Ca^{2+} and ROS: Flow cytometric analysis of mitochondria was performed using a BD LSR Fortessa equipped with a 488 nm argon laser and a 635 nm red diode laser (BD LSR Fortessa, Jose, CA). Data from the experiments were analyzed using the FlowJo software (BD Bioscience, San Jose, CA). To exclude cell debris, the samples were gated based on light-scattering properties in the side scattering and forward scattering modes, and 100,000 events per sample within the R1 gate (mitochondrial population) were collected. For staining, each mitochondrial sample equivalent to 50 µg protein was suspended in the analysis buffer (250 mmol/L sucrose, 20 mmol/L 3-(N-morpholino) propanesulfonic acid (MOPS), 10 mmol/L Tris- Base, 100 µmol/L, and 0.5 mmol/L magnesium chloride ($MgCl_2$) and 5 mmol/L succinate at pH 7.4). To measure mitochondrial membrane potential, they were stained with 100 nmol/L TMRM (Tetramethylrhodamine Methyl ester, Thermofisher Scientific, Waltham, MA; excitation at 548 nm and emission at 574 nm). To measure mitochondrial Ca^{2+}, they were stained with 50 µm/L Fluo-4 (excitation at 494 nm and emission at 506 nm, Thermofisher Scientific), and to measure mitochondrial ROS, they were stained with 10 mmol/L H2DCFDA (2′,7′-dichlorofluorescein diacetate, Thermofisher Scientific; excitation at 492 nm and emission at 525 nm).

Mitochondrial ATP production: In a separate group of animals, mitochondria isolated as above were analyzed for ATP production capacity using luciferase-based assay (Life Technologies, Catalog number: A22066). In brief, to each 10 µl of mitochondria samples in 96 well plates, 100 µl of the reaction solution was added and luminescence signal was measured at 5 min using a microplate reader (Cytation5 BioTek Instruments, Inc., Winooski, VT). A standard plot with different amount of ATP was created ($R^2 = 0.98$) at the same time, and was used to calculate

ATP produced by mitochondrial samples from luminescence signal. The ATP data were normalized to mitochondrial protein levels.

Immunohistochemistry: In a separate group of animals, spinal cords were analyzed for different markers. For this, the spinal cords centered at the injury site were dissected from the vertebral canal and post-fixed in 4% PFA at room temperature for ~48 hrs; they were then placed into 70% ethanol (Pharmco-AAPER, Brookfield, CT) and kept at 4 °C until standard processing and embedding in paraffin. The spinal cords were trimmed to ~2 cm sections that included the lesion site and were then embedded in a paraffin block. The spinal cord blocks were sectioned with a microtome (Leica RM2135, Buffalo Grove, IL) at 10 µm on the longitudinal plane and mounted on Superfrost Plus Microscope slides (Fisher Scientific, Pittsburgh, PA). For immunofluorescence staining, spinal cord sections were deparaffinized in xylene (Sigma) and rehydrated in gradient dilutions of ethanol-water (100, 90, 70, 50%) for two minutes in each. The sections were then unmasked in boiling 10 mM sodium citrate buffer with 0.05% Tween-20 (Sigma) for 30 min. After cooling down and washing, the sections were blocked in a blocking serum solution (1% BSA in 1X PBS/5% normal serum/ 0.3% Triton X-100) for 60 min. The blocked sections were then incubated with primary antibodies in blocking solution overnight at 4 °C. The primary antibodies were as follows: Cleaved Caspase-3, Rabbit (1:200 dilution, Cat# 9661, Cell Signaling Technology, Danvers, MA) and anti-cytochrome C antibody, Mouse monoclonal (1:200 dilution, Cat# ab13575, Abcam, Cambridge, MA). The secondary antibodies were incubated in RT for 1-2 hr with goat anti-rabbit (1:500 dilution, Cat# (Alexa Fluor 488 Conjugate, Cat #4412, Cell Signaling Technology) and goat anti-mouse (1:500 dilution, Fluro-488, Cat# ab150117, Abcam). For ROS, the slides were stained with DHE (Dihydroethidium, Thermofisher Scientific) for 30 min at room temperature followed by washing five times with 1X PBS. Slides were then mounted and counterstained with VECTASHIELD mounting media with DAPI (Cat# H1200, Vector Laboratories, Burlingame, CA). The sections were scanned at 20x magnification with a Leica DM6B upright microscope scanner equipped with a Leica DFC 7000T camera and LAS X software (Leica Microsystems, GmbH, Wetzlar, Germany).

TUNEL Assay: For TUNEL staining (Thermofisher Scientific), the spinal cord sections were deparaffinized in xylene and rehydrated in ethanol (as described above) followed by immersing slides twice in 1X PBS for 5 min each. The slides were incubated in sufficient volume of the permeabilization reagent (Proteinase K solution) for 15 min. After that, the slides were washed twice in PBS for 5 min each and incubated in 100 µl of TdT Reaction Buffer (Component A). After 10 min, the TdT Reaction Buffer was removed and 50 µl of the prepared TdT reaction mixture (TdT reaction buffer+ EdUTP + TdT enzyme) was added on to each slide and incubated for 60 min at 37 °C. The slides were washed with the 3% BSA and 0.1% Triton X-100 in PBS for 5 minutes and added with 50 µl of the Click-iT™ Plus TUNEL reaction cocktail to each slide to allow the solution to spread completely over the surface for 30 min at 37 °C. Click-iT™ Plus TUNEL reaction cocktail was removed, the slides were washed with 3% BSA in PBS for 5 min. After mounting and counterstaining with VECTASHIELD mounting media with DAPI (Cat# H1200, Vector Laboratories, Burlingame, CA), the sections were scanned at 20x magnification with a Leica DM6B upright microscope scanner equipped with a Leica DFC 7000T camera and LAS X software (Leica Microsystems, GmbH, Wetzlar, Germany).

Quantification: For quantifications, images were captured on at least three sections from 4-6 different animals. Analyses were performed by comparing changes in the fixed-size target area in different groups. Three different areas (3 mm^2) were analyzed from each section involving the entire spinal cord by using tools of ImageJ 1.46r (ImageJ, NIH, Bethesda, MD). The positively stained cells were counted using the plugin cell counter of ImageJ. To calculate the percentage of TUNEL, caspase-3 and cytochrome-c positive cells, total number of DAPI stained cells were counted using the same ImageJ software. For calculating the percentage of positive cells in the entire spinal cord, sections 6 mm length x 3 mm width were selected, while the calculating percentage of positive cells at the impact site, an area of (2 mm^2) at the lesion site, was taken. The sections were split in different color channels (Blue, Red and Green), followed by thresholding to count the positive cells in their respective channels.

Statistical analyses: All the data were analyzed as mean ± standard error of the mean (s.e.m.). The statistical significance between the groups was determined by using GraphPad Prism 7.04 software (GraphPad Software Inc., San Diego, CA) for one-way analysis of variance (ANOVA) and Student's t-test. Values of $p<0.05$ were considered significant

Results

Physical characterization of nano-SOD/CAT. The mean hydrodynamic diameter of nano-SOD/CAT was 293 ± 6.4 nm (n=11) (Figure 1A) with polydispersity index of 0.065 ± 0.005 (n=11) and zeta potential of -17.1 ± 1.5 mV (n=10). The polydispersity index <0.1 indicates uniform particle size distribution. The TEM picture of nano-SOD/CAT shows circular structures with a mean diameter of 122 ± 5.5 nm (n=100) (Figure 1B). Activity of SOD used in the formulation was 5,605 ± 12 U/mg and that of catalase was 4860 ± 41 U/mg. The encapsulation efficiency of SOD was 73 ± 4.6%, whereas that of CAT was 85.2 ± 3.1% (mean ± s.e.m, n=3). Based on the encapsulation efficiencies, each mg of nano-SOD/CAT contained 749.9 ± 5.6 units or ~133 µg of SOD and 814.6 ± 3.5 units or ~167 µg of CAT. The cumulative release of SOD was 44.4 ± 3.5%, whereas that of CAT was 60.1 ± 3.2 % in 7 days (Figure 1C and D).

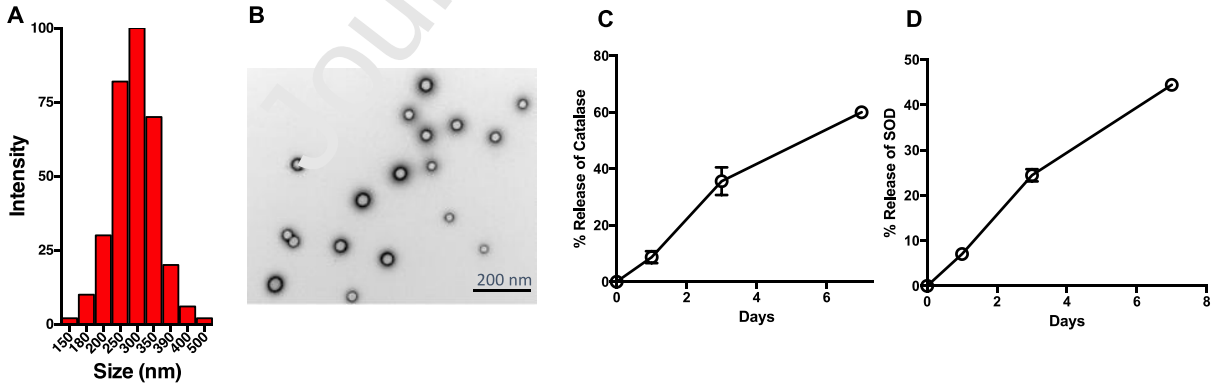

Figure 1: Physical characterization of nano-SOD/CAT and release: A) Hydrodynamic size distribution of nano-SOD/CAT as measured in water using dynamic light scattering technique, **B)** TEM picture of nano-SOD/CAT, and *in vitro* release of **C)** catalase and **D)** superoxide dismutase from nano-SOD/CAT under *in vitro* conditions. Release study was carried out in PBS buffer containing BSA and Tween-80 at 37 ºC. The released enzyme levels were quantified using the respective assay kits and the data are plotted as cumulative percent release (Data as mean ± s.e.m., n = 3).

Spinal cord injury. The average weight of rats (male/female) prior to injury was 327.5 ± 5 g. The average impact force was 249.7 ± 3.4 Kdyn and the speed of impactor was 120.3 ± 4.9 mm/s. All the animals developed complete paraplegia following SCI. There was no animal mortality during the experimental period in any of the groups.

Mitochondrial analysis. Flow cytometric analysis of the mitochondria isolated from the spinal cords at 1-wk post-SCI from the untreated control group showed 39 ± 1.5% reduction in MMP (Figure 2A), 169 ± 2.1% increase in ROS levels (Figure 2B), and 46 ± 1.5% increase in Ca^{2+} (Figure 2C) as compared to the levels in the mitochondria isolated from the spinal cords of sham control animals. These results thus clearly indicate mitochondrial dysfunction following the injury. Analysis of the mitochondria isolated from the spinal cords of treated animals showed partial reversal in the above parameters. For example, MMP of the mitochondrial isolated from the spinal cords of the treated group showed an increase of 33 ± 0.9% as compared to those isolated from the spinal cords of untreated control, but remained 19 ± 1.9% lower than that of the mitochondria isolated from the spinal cords of sham control animals. A similar trend was seen in the mitochondrial ROS (Figure 2B) and Ca^{2+} levels (Figure 2C) in treated vs. untreated controls and sham control (Figure 2). The animals treated with SOD/CAT in solution did not show significant protective effect on mitochondria as the results were similar to those from untreated control.

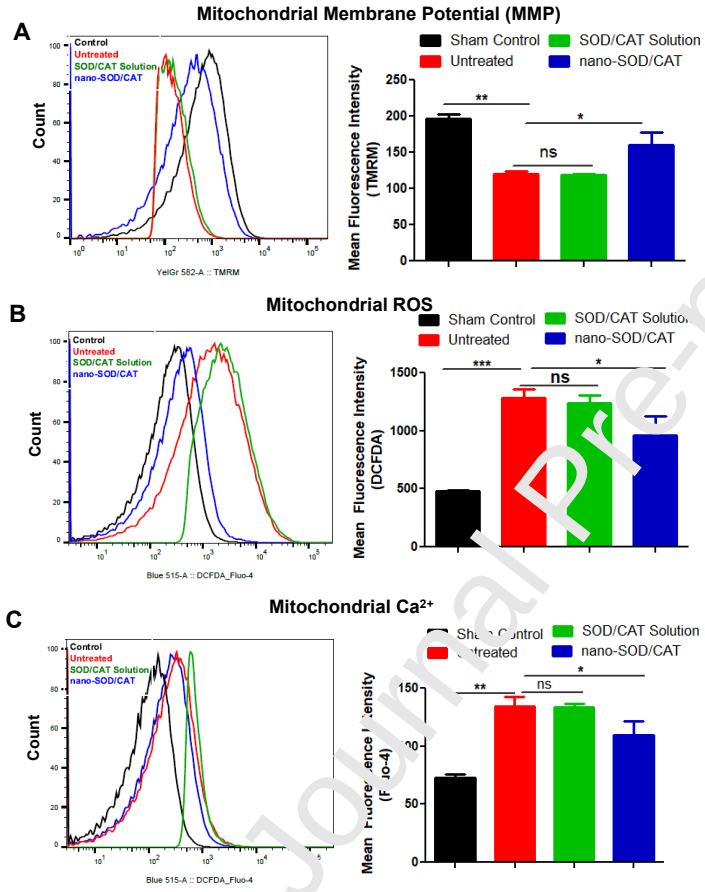

Figure 2: Analysis of mitochondrial function following treatment with nano-SOD/CAT. At 6 hrs post-SCI, the animals were administered a single intravenous dose of nano-SOD/CAT or SOD/CAT in solution. Mitochondrial isolated after 1-wk from the impacted region of the spinal cord were characterized using flow cytometry and the results were compared with the mitochondria isolated from the spinal cords of untreated and sham control animals. **A)** Mitochondrial membrane potential, **B)** Mitochondrial ROS, **C)** Mitochondrial Ca^{2+}. Mitochondria isolated from the spinal cords of the treated animals show an increase in mitochondrial membrane potential, reduced ROS and Ca^{2+} as compared with the mitochondria isolated from the spinal cords of untreated control. ***P<0.001 and **P<0.01 sham control vs untreated, *P<0.05 untreated vs nano-SOD/CAT treated, ns = not significant (Data as mean ± s.e.m., n = 4-6).

The mitochondria isolated from the spinal cords of treated animals showed higher ATP production capacity as compared with those isolated from the spinal cords of untreated controls, but remained lower than ATP production capacity of the mitochondria isolated from the spinal

cords of sham control animals (Figure 3). The overall results thus indicate that the treatment partially mitigated mitochondrial dysfunction that occurred after SCI.

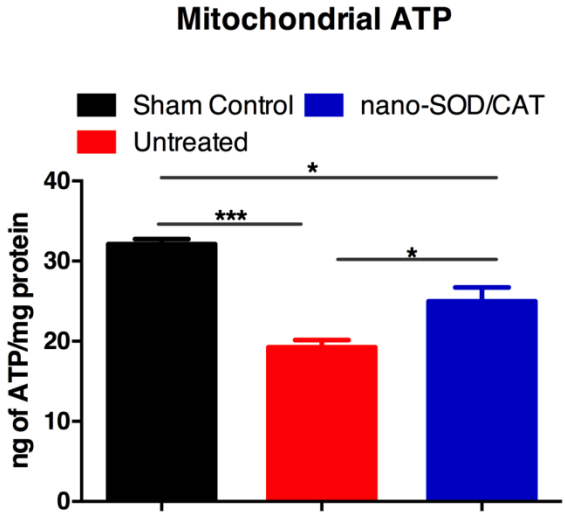

Figure 3: Effect of treatment on ATP production capacity. At 6 hrs post-SCI, the animals were given a single intravenous dose of nano-SOD/CAT. Spinal cords were collected 1-wk post treatment, and mitochondria was isolated to determine ATP production capacity. The spinal cords of treated animals show more ATP production capacity as compared with the mitochondria isolated from the spinal cords of untreated control but remained lower than those isolated from the sham control animals. ***P<0.001 sham control versus untreated *P<0.05 untreated vs treated (Data as mean ± s.e.m., n=3).

Activation/release of apoptotic factors. Mitochondrial dysfunction after SCI is characterized by activation of apoptotic factors, particularly cytochrome c and activation of caspase-3. In addition, ROS are released from dysfunctional mitochondria that have been known to have damaging effects on cell proteins, DNA and membrane lipids [17]. Histological analysis of the spinal cords from treated animals showed significantly reduced levels in all the above markers as compared to the spinal cords of untreated animals (Figure 4). This observation is consistent when the data are computed for percent of positive cells over the total number of cells counted in histological sections (Table 1). The spinal cord sections from sham control animals show no significant ROS activity or presence of cytochrome c and caspase-3 positive cells (Figure 4, Table 1).

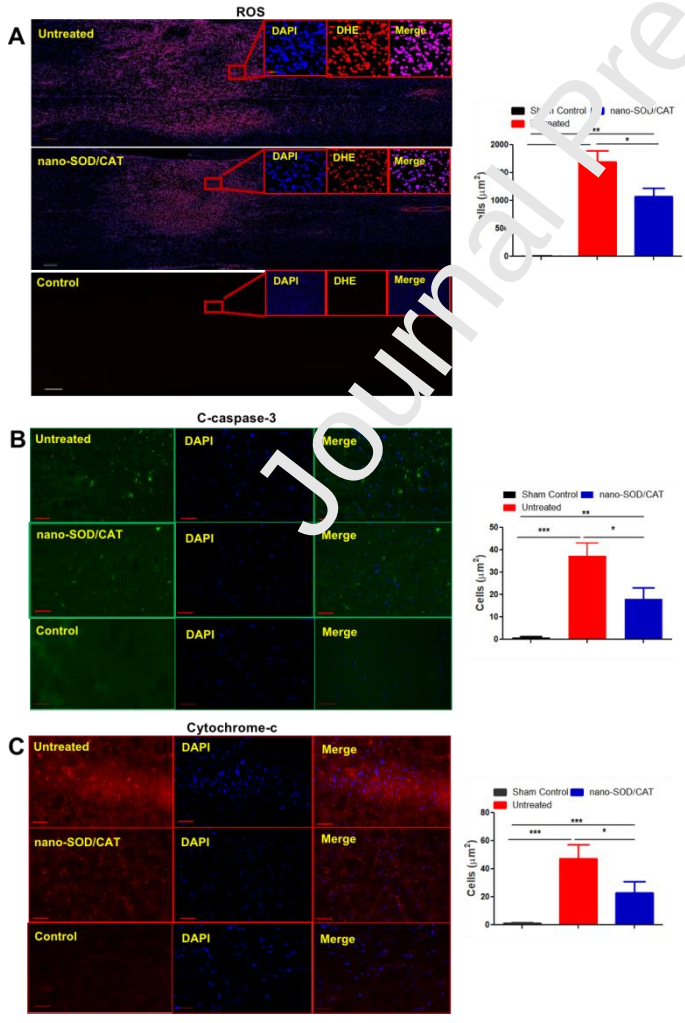

Figure 4: Characterization of spinal cords for ROS and apoptotic factors following treatment with nano-SOD/CAT. At 6 hrs post-SCI, animals were given a single intravenous dose of nano-SOD/CAT and the spinal cords were collected 1-wk post treatment for immunohistochemical analysis. **A)** ROS activity in spinal cord following treatment with nano-SOD/CAT. The sections were analyzed for ROS

using DHE staining. The sections taken from treated animals shows less ROS as compared with the sections taken from the spinal cords of untreated control. The spinal cord sections of sham control animals show insignificant ROS activity. *P<0.05 untreated versus treated (Data as mean ± s.e.m., n=6). Scale bar = 200 µm and magnification = 20x. **B)** Inhibition of activation of caspase-3 in nano-SOD/CAT treated animals. The spinal cord sections were stained with cleaved caspase-3. The sections taken from treated animals shows reduced number of caspase-3 cells as compared to the sections taken from the spinal cords of untreated control. ***P<0.001 sham control versus untreated, *P<0.05 untreated versus treated (Data as mean ± s.e.m., n=4). Scale bar = 100 µm and magnification = 20x. **C)** Inhibition of cytochrome c release in treated animals. The spinal cord sections were stained with cytochrome c antibody. The spinal cords of the treated animals show reduced number of cytochrome cells as compared with the spinal cords of untreated control. ***P<0.001 sham control vs untreated *P<0.05 untreated vs treated (Data as mean ± s.e.m., n=4). Scale bar = 100 µm and magnification = 20x

Apoptosis: SCI increases ROS levels and apoptotic factors that lead to neuronal cell death. Our data show significantly reduced number of apoptotic cells in the spinal cords of treated animals as compared with the spinal cords of untreated control. Compared to untreated and treated groups, the spinal cords of sham control animals show very few TUNEL-positive cells (Figure 5). This observation is consistent when the data are computed for TUNEL-positive cells per mm^2 area (Figure 5) or percent of TUNEL positive cells over total number of cells counted in the entire spinal cord section (6 x 3 mm) or the area of 2 mm^2 at the lesion site (Table 1).

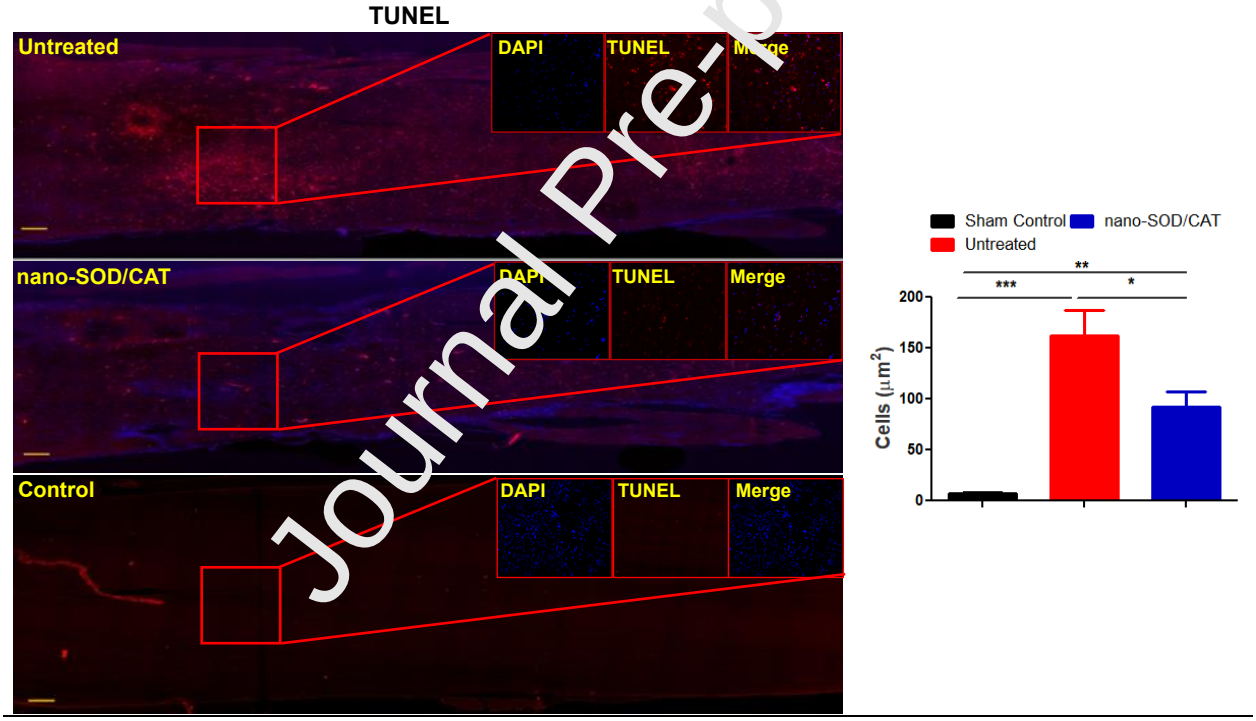

Figure 5: Protective effect of nano-SOD/CAT treatment on apoptosis. At 6 hrs post-SCI, the animals were given a single intravenous dose of nano-SOD/CAT. Spinal cords were collected 1-wk post-treatment and the sections were stained for TUNEL. The spinal cords of treated animals show reduced number of TUNEL cells as compared with the spinal cords of untreated control. ***P<0.001 sham control versus untreated *P<0.05 untreated vs treated (Data as mean ± s.e.m., n=6). Scale bar = 200 µm and magnification = 20x

Lesion area, body weight loss, and BBB score. Visual observation of the spinal cords of treated animals show reduced lesion area as compared with the spinal cords of untreated controls. In addition, the treated animals showed lower weight loss than untreated control animals. The BBB score of treated animals at 1 wk was higher than that of the untreated control animals (Figure 6).

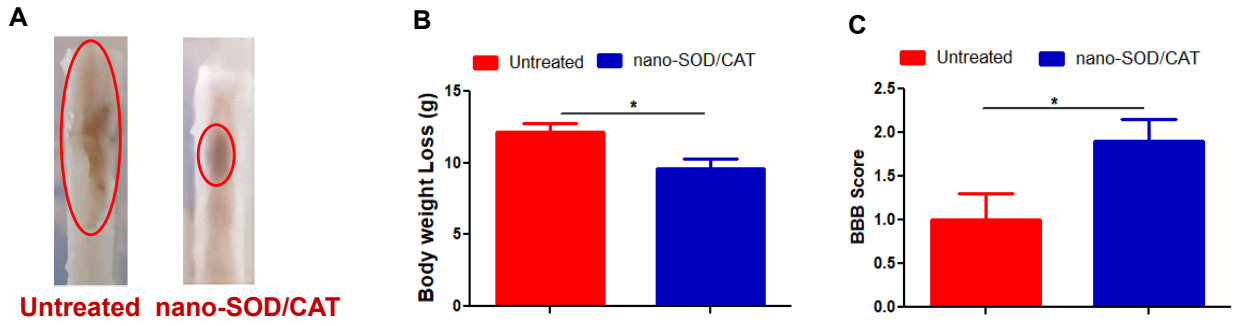

Figure 6: Effect of treatment on lesion area, body weight loss and BBB score. Animals were given a single intravenous dose of nano-SOD/CAT, at 6 hrs post-SCI, and data were collected at 1 wk. The spinal cords of the treated animals show **A)** smaller lesion area, **B)** lower body weight loss, C) improved BBB scores than untreated animals. Image of the lesion area is representative images of spinal cord of untreated and treated animals. Body weight and BBB, $*P<0.05$ Untreated vs treated (Data as mean ± s.e.m., n = 10).

Table 1: Effect of nano-SOD/CAT treatment on percent cells expressing apoptotic factors and apoptotic cells in spinal cord at 1 wk

Groups	Sham Control		Untreated		Treated	
Markers	Entire Spinal Cord Section	Epicenter	Entire Spinal Cord Section	Epicenter	Entire Spinal Cord Section	Epicenter
C-caspase-3$^+$ (%)	0	0	18.1 ± 1.3	15.3 ± 3.15	7.3 ± 1.3***	5.2 ± 2.2$^{###}$
Cytochrome-c$^+$ (%)	0	0	21.2 ± 2.3	29.3 ± 3.4 ††	11.5 ± 2.4**	15.4 ± 2.7$^{##}$
TUNEL$^+$ (%)	1.2	0	23.1 ± 1.2	47.8 ± 1.2 †††	11.8 ± 3.7**	23.4 ± 3.1$^{###}$, †††

Data as mean ± s.e.m, n= 4-6. ***$p < 0.001$, **$p < 0.01$ Untreated vs. Treated (Entire spinal cord section), $^{###}p < 0.001$, $^{##}p < 0.01$ Untreated vs. Treated (Epicenter), ††† $p < 0.001$, †† $p < 0.01$ Entire spinal cord vs. Epicenter.

Discussion

There is a growing quest to find an effective therapeutic intervention that can be administered as soon as possible after SCI to protect it from rapidly progressing, degenerating secondary injury cascades. The intention is not only to minimize severity of the post-injury disability but also to enhance the prospects of achieving better neurological and functional recovery. Although the secondary injury cascade is quite complex and dynamic in nature, and several mechanisms have been proposed for its progression, the loss of mitochondrial homeostasis after SCI is well recognized [18, 19]. Mitochondrial dysfunction after the injury causes oxidative stress that leads to the release of ROS and activation of other apoptotic factors [20]. The ultimate effect is more spinal cord neuronal cell death with time, in addition to that is caused by the primary injury, triggering a greater inflammatory response and initiation of a sequential chain of degenerative events that affect not only the impacted site but also the spinal cord distant to the lesion site [21]. The increased inflammatory response with degeneration of the spinal cord also affects other organs, not only because of the greater loss of neuronal connectivity with time but also due to increasing levels of systemic proinflammatory cytokines, inflammatory cells, and ROS [22]. Thus, protecting mitochondria after the injury becomes a logical step in mitigating the overall impact of the primary injury response.

As described under the method section, nano-SOD and nano-CAT were formulated separately and combined in 1:2 w/w ratio at a later stage during the recovery process and prior to

lyophilization. This way the two enzymes do not compete for encapsulating into the same nanoparticle polymer mextrix. As expected, the mean hydrodynamic diameter of nano-SOD/CAT was larger than the TEM diameter (293 ± 6.4 nm vs. 122 ± 5.5 nm). This is because hydrodynamic diameter is measured in an aqueous phase where hydration of the surface associated PVA (referred to as residual PVA) also contributes towards the overall diameter [23] whereas the TEM diameter is measured in a dry state. We have previously reported discrepancy in hydrodynamic and TEM diameters of PLGA-based NPs [24]. In the formulation of nano-SOD/CAT, BSA was used as an inert bulking protein that helps in the encapsulation of enzymes and protects them from interfacial activation [15, 25]. DMT was used as an inert plasticizer and pore-forming agent that prevents accumulation of acidic oligomers within NPs that are formed as a result of polymer degradation; if these acidic oligomers remain entrapped in NPs, they can potentially denature proteins [26]. Also, because DMT forms pores, it helps in the release of the encapsulated enzymes in a sustained manner in active form [14]. Our data show that the release of CAT is faster than SOD (cumulative release 60% vs. 45% in 7 days) which could be due to differences in their molecular weight (CAT = 240 Kd vs. SOD = 32.5 Kd) and higher CAT loading than SOD per mg of nano-SOD/CAT. We did not achieve 100% release of enzymes as some of it may have degraded during the release at 37 ºC. At 28 days, the cumulative release of SOD was 77 ± 2.5% while that of CAT was 84 ± 3.5% and the release did not change thereafter.

Mitochondria are double-membrane organelles. The outer bilipid membrane, which contains voltage-dependent anion channels, regulates the transport of nucleotides, ions and metabolites, while the inner membrane, which is more complex, regulates ETC to maintain the necessary electrochemical gradient for ATP synthesis [27]. The significant drop in MMP following SCI seen in our study indicates depolarization of the mitochondrial membrane (Figure 2A), leading to the opening of the ion channels that results in the influx of calcium (Figure 2C). Calcium overload increases the production of various ROS (e.g., superoxide anion, hydrogen peroxide, and hydroxyl radicals) (Figure 2B) [28]. Our data show all of the above characteristics in mitochondria isolated from the spinal cords of untreated control; however, those isolated from the spinal cords of the nano-SOD/CAT treated animals show a partial reversal in these parameters (Figure 2). This reversal is also evident from the reduced mitochondrial ROS levels, increased MMP, and reduced mitochondrial calcium levels in treated group than in untreated control. The effect of treatment was seen from the ability of the mitochondria isolated from the spinal cords of treated group to produce more ATP than those isolated from the spinal cords of untreated control (Figure 3). Although the treatment did not regain the same mitochondrial function or ATP production capacity as those isolated from the spinal cords of uninjured sham control animals, it significantly attenuated the post-injury mitochondrial dysfunction.

Reduction in MMP after SCI can lead to a series of changes in the inner and outer mitochondrial membrane, such as the release of cytochrome c, ROS, and activation of caspase family members, leading to neuronal cell apoptosis [29]. Immunohistochemical analysis shows that there is a significant reduction in cytochrome c translocation, cleaved caspase-3, and ROS activities in the spinal cords of treated vs. untreated animals (Figure 4). Inhibiting the translocation of cytochrome c is also possible due to a decrease in mitochondria membrane permeabilization, suggesting the role of nano-SOD/CAT in stabilizing the mitochondrial membrane. The ultimate effect of the treatment can be seen from reduced neuronal cell apoptosis in the spinal cords of treated animals compared with untreated control (Figure 5). Further, the spinal cords of treated

animals show reduced lesion than that in untreated control, an indication of inhibition of expansion of the secondary injury cascades following nano-SOD/CAT treatment (Figure 6A).

Overall data support our hypothesis that the treatment with nano-SOD/CAT mitigated the mitochondrial dysfunction, and hence the release of ROS and activation apoptotic factors (Figure 4), thus protecting the spinal cord from apoptosis (Figure 5). Relatively lower weight loss in treated animals vs. untreated control reflects the improvement in overall animal health following treatment (Figure 6B). Due to reduced secondary injury response in treated animals, it may have improved the overall metabolic activity of these animals. Treated animals also demonstrated a better locomotive function (as reflected in the BBB score) than untreated control, which is an indication of a trend towards functional recovery (Figure 6C). The treatment effect can be linked to high ATP production capacity of the mitochondria isolated from the spinal cords of treated animals over untreated animals (Figure 3). It is well recognized that mitochondria behave as intracellular signal-processing networks [30] and can promote neurogenesis [31]. Hence, a long-term study is needed to see how far the treatment effect goes in achieving the BBB score of 21 (the score of the sham control animals). Such a study would also require further optimization of dose and dosing frequency of nano-SOD/CAT treatment. In this study, we used nano-SOD and nano-CAT in 1:2 ratio which is based on the efficacy of this composition in our previous thromboembolic stroke model [32]. However, it would be interest to determine what composition of enzymes in nano-SOD/CAT formulation has the most protective effect on injured spinal cord.

The compounds with antioxidant properties, free radical scavengers, and mitochondrial protective agents have been tested; however, clinical translation of these agents has yet to be achieved [3]. The inefficacy of these agents has been attributed to their low potency to neutralize excessive ROS produced at the lesion site. Further, their biodistribution to other organs and short half-lives limited their uptake by the spinal cord to cause any significant effect on mitochondria. The main advantage of using antioxidant enzymes is their catalytic activity, which makes them very effective in neutralizing ROS [15]. However, antioxidant enzymes as such, are not effective due to their very short half-lives *in vivo* ($t_{1/2}$ of SOD in rats = 4-8 min, CAT = 8-10 min). This could explain the inefficacy of the SOD/CAT solution treated animals in protecting mitochondria following the injury (Figure 2). PEGylation increases half-life, but the modified enzymes are not effective in cellular and tissue uptake [33]. Although a small fraction of the administered nano-SOD/CAT localizes at the lesion site (0.13% or 10.5 µg NPs at 24 hrs, 30 mg/kg dose administered 6 hr post-injury), it can form a depot at the lesion site [13]. Thus, the nano-SOD/CAT localized at the lesion can provide a sustained and localized protective effect of antioxidant enzymes that are catalytic in action, and hence are potent and effective in neutralizing ROS. Recently, Anderson et al. [34] have shown that direct injection of a combination of growth factors into the spinal cord at a fraction of microgram levels in 0.25 µl gel was effective in inducing neurogenesis in rat SCI model. Hence, critical for the efficacy of the treatment that is administered intravenously in SCI is high potency of the agent delivered at target area which, in this case, are antioxidant enzymes due to their catalytic activity and the nano-SOD/CAT localized at the lesion site making a depot effect. In this case, a major fraction of the administered nano-SOD/CAT would distribute to other organs but with nano-SOD/CAT, it could provide protective effect to those organs from the increased systemic ROS levels and inflammatory response that occur after the injury [22]. Less bodyweight loss in the treated group as compared to untreated group could also be due to the protective effect of nano-SOD/CAT to

other organs. As SOD and CAT are present in normal tissue, their nonspecific distribution, unlike other drugs (e.g., methylprednisone) [35], is not expected to cause side effects.

The possible mechanism of efficacy of nano-SOD/CAT treatment could be the improvement in the mitochondrial respiratory chain components that are compromised due to the formation of excess ROS after the injury (Figure 7). Although not determined in our study, another secondary event after SCI is depolarization and opening of voltage-dependent ion channels, leading to the release of excitatory neurotransmitters, such as glutamate [36]. Glutamate binds to glutamate receptors, especially N-methyl-D-aspartate, and results in accumulation of Ca^{2+} inside the mitochondria above a threshold level that triggers the opening of the mitochondrial permeability transition pore (mPTP) and the influx of Ca^{2+} in mitochondria [37]. At cellular level, nano-SOD/CAT taken up by cells can neutralize the ROS already released by mitochondria, which in turn can impact the mitochondrial ROS levels (Figure 4A), thus stabilizing them from oxidative stress and preventing further release of ROS and other apoptotic factors. Thus, nano-SOD/CAT localized at the lesion site can break the vicious cycle of degeneration by protecting mitochondria. The impact of this mechanism is clearly evident from reduced neuronal cell death in treated animals (Figure 5).

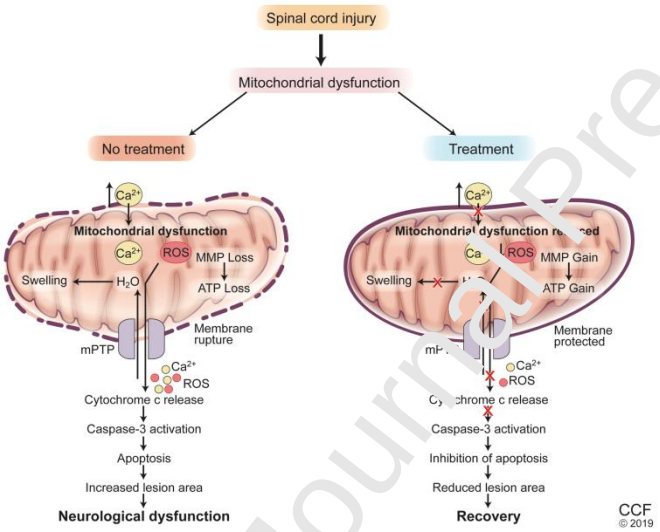

Figure 7: Schematic depicting the mechanism of efficacy of treatment with nano-SOD/CAT: The treatment attenuated production of mitochondrial ROS and inhibited Ca^{2+} influx, which in turn inhibited the mitochondrial membrane permeabilization. Treatment inhibited the formation of mPTP, eventually blocking the translocation of cytochrome *c* from mitochondria to cytosol, activation of caspase-3 and swelling of mitochondria. These effects partially restored the MMP and regained ATP production capacity of mitochondria. The combined effect was inhibition of spinal neuronal apoptosis, reduce lesion site and better recovery with treatment as compared to in untreated control.

With time, degenerative effect of the secondary injury spreads from the impacted region to the distal segments of the spinal cord, which are not affected by the impact. The upregulation of caspases in rostral and caudal segments that are away from the lesion site is considered responsible for the long-term neurological deficits after SCI [38]. Hence, a future study could focus on determining how protecting the lesion site affects the activation of apoptotic pathways in spinal cord segments distant from the injury site. Dysfunctional mitochondria are also linked to neuroinflammation [39], and hence, protecting mitochondria could have reduced the inflammation-mediated damage to the spinal cord.

It would be of interest to determine what types of macrophages (inflammatory M1 vs. pro-regenerative M2) accumulate at the lesion site in the nano-SOD/CAT treated group as compared to in untreated control and the potential role they might play in shifting the balance towards regeneration rather than degeneration of the spinal cord [40]. The oxidative-stress free

enviornment at the lesion site in the treated group potentially could promote the healing process by selective differentiation of macrophages to pro-regenerative M2 macrophage phenotype. Future studies could also involve determining the dose-response effect, an optimal time window for treatment, and long-term outcome of the treatment effect to support the notion that an effective early therapeutic intervention can lead to better long-term neurological and functional recovery.

Since nano-SOD/CAT is an intravenous treatment, it can be administered on-site or *en route* to a trauma center to prevent further degeneration of the spinal cord. In this study, we selected treatment 6 hrs post-injury, which provides a wide window for the treatment. Most other preclinical studies were carried out at significantly earlier time points (prior to, immediately or >3 hrs post-injury), thus missing the clinical relevance of the study. We anticipate that the treatment effect with nano-SOD/CAT can be much better if it is given sooner after the injury. Since ROS continue to produce beyond 6 hrs, it is also possible that nano-SOD/CAT treatment could be effective beyond the time window we tested. However, this would also depend on what other degenerating factors, such as inflammation and other degenerating cascades, play a dominating role with time delay.

Conclusions

Our results demonstrate that SCI results in mitochondrial dysfunction, and the treatment with antioxidant enzymes formulated in nano-SOD/CAT protects mitochondria, reduces ROS activities, prevents the release of cytochrome c, and inhibits activation of caspase-3. The overall effect of the treatment is protecting the spinal cord from neuronal cell apoptosis and further degeneration. Nano-SOD/CAT thus can be explored for early therapeutic intervention to minimize the impact of primary injury response and achieve better neurological and functional recovery with time.

Acknowledgment

This work was supported by the National Institute of Neurological Disorders and Stroke of the National Institutes of Health under Grant R01NS092033, and the Department of Defense, through the Spinal Cord Injury Research Program, under Award No. W81XWH-16-1-0786. Opinions, interpretation, conclusions and recommendations are those of the authors and are not necessarily endorsed by the Department of Defense.

Author's contribution

SA: Animal study, nano-SOD/CAT characterization, mitochondrial analysis, immunohistochemical analysis, behavior study, data analysis, and manuscript writing; **JY:** Animal procedure, immunohistochemical analysis, behavior study, and manuscript writing; **YG:** Animal procedure; **YK:** nano-SOD/CAT formulation and characterization and behavior study; and **VL:** Conceptualization, study design and supervision, data analysis and intepretation, and manuscript writing.

Conflict of interest

VL is a co-inventor on pending US and EU patents for the use of antioxidant nanoparticles for treating spinal cord injury. The conflict of interest is managed by the Conflict of Interest Committee of Cleveland Clinic according to its conflict of interest policies.

Bibliography

[1] N.D. James, S.B. McMahon, E.C. Field-Fote, E.J. Bradbury, Neuromodulation in the restoration of function after spinal cord injury, Lancet Neurol, 17 (2018) 905-917.

[2] L.C. O'Brien, A.S. Gorgey, Skeletal muscle mitochondrial health and spinal cord injury, World J Orthop, 7 (2016) 628-637.

[3] N.E. Scholpa, R.G. Schnellmann, Mitochondrial-Based Therapeutics for the Treatment of Spinal Cord Injury: Mitochondrial Biogenesis as a Potential Pharmacological Target, J Pharmacol Exp Ther, 363 (2017) 303-313.

[4] A.S. Gorgey, O. Witt, L. O'Brien, C. Cardozo, Q. Chen, E.J. Lesnefsky, Z.A. Graham, Mitochondrial health and muscle plasticity after spinal cord injury, Eur J Appl Physiol, 119 (2019) 315-331.

[5] P.G. Sullivan, A.G. Rabchevsky, P.C. Waldmeier, J.E. Springer, Mitochondrial permeability transition in CNS trauma: cause or effect of neuronal cell death?, J Neurosci Res, 79 (2005) 231-239.

[6] Z. Jia, H. Zhu, J. Li, X. Wang, H. Misra, Y. Li, Oxidative stress in spinal cord injury and antioxidant-based intervention, Spinal Cord, 50 (2012) 264-274.

[7] M. Mittal, M.R. Siddiqui, K. Tran, S.P. Reddy, A.B. Malik, Reactive oxygen species in inflammation and tissue injury, Antioxid Redox Signal, 20 (2014) 1126-1167.

[8] A. Bobba, G. Amadoro, D. Valenti, V. Corsetti, P. Lassandro, A. Atlante, Mitochondrial respiratory chain Complexes I and IV are impaired by beta-amyloid via direct interaction and through Complex I-dependent ROS production, respectively, Mitochondrion, 13 (2013) 298-311.

[9] A. Grimm, A. Eckert, Brain aging and neurodegeneration: from a mitochondrial point of view, J Neurochem, 143 (2017) 418-431.

[10] E. Birben, U.M. Sahiner, C. Sackesen, S. Erzurum, O. Kalayci, Oxidative stress and antioxidant defense, World Allergy Organ J, 5 (2012) 9-19.

[11] A.E. Mautes, M.R. Weinzierl, F. Donovan, L.J. Noble, Vascular events after spinal cord injury: contribution to secondary pathogenesis, Phys Ther, 80 (2000) 673-687.

[12] J.C. Fleming, M.D. Norenberg, D.A. Ramsay, G.A. Dekaban, A.E. Marcillo, A.D. Saenz, M. Pasquale-Styles, W.D. Dietrich, L.C. Weaver, The cellular inflammatory response in human spinal cords after injury, Brain, 129 (2006) 3249-3269.

[13] Y. Gao, S. Vijayaraghavalu, M. Stees, B.K. Kwon, V. Labhasetwar, Evaluating accessibility of intravenously administered nanoparticles at the lesion site in rat and pig contusion models of spinal cord injury, J Control Release, 302 (2019) 160-168.

[14] M.K. Reddy, V. Labhasetwar, Nanoparticle-mediated delivery of superoxide dismutase to the brain: an effective strategy to reduce ischemia-reperfusion injury, Faseb J, 23 (2009) 1384-1395.

[15] M.K. Reddy, L. Wu, W. Kou, A. Ghorpade, V. Labhasetwar, Superoxide dismutase-loaded PLGA nanoparticles protect cultured human neurons under oxidative stress, Appl Biochem Biotechnol, 151 (2008) 565-577.

[16] D.M. Basso, M.S. Beattie, J.C. Bresnahan, Graded histological and locomotor outcomes after spinal cord contusion using the NYU weight-drop device versus transection, Exp Neurol, 139 (1996) 244-256.

[17] A. Singh, R. Kukreti, L. Saso, S. Kukreti, Oxidative stress: A key modulator in neurodegenerative diseases, Molecules, 24 (2019) 1583.

[18] C.S. Ahuja, S. Nori, L. Tetreault, J. Wilson, B. Kwon, J. Harrop, D. Choi, M.G. Fehlings, Traumatic spinal cord injury-repair and regeneration, Neurosurgery, 80 (2017) S9-s22.
[19] M.A. Anwar, T.S. Al Shehabi, A.H. Eid, Inflammogenesis of Secondary Spinal Cord Injury, Front Cell Neurosci, 10 (2016) 98.
[20] D. Sobrido-Camean, A. Barreiro-Iglesias, Role of Caspase-8 and Fas in Cell Death After Spinal Cord Injury, Front Mol Neurosci, 11 (2018) 101.
[21] N. Zhang, Y. Yin, S.J. Xu, Y.P. Wu, W.S. Chen, Inflammation & apoptosis in spinal cord injury, Indian J Med Res, 135 (2012) 287-296.
[22] Y.O. Mukhamedshina, E.R. Akhmetzyanova, E.V. Martynova, S.F. Khaiboullina, L.R. Galieva, A.A. Rizvanov, Systemic and Local Cytokine Profile following Spinal Cord Injury in Rats: A Multiplex Analysis, Front Neurol, 8 (2017) 581.
[23] S.K. Sahoo, J. Panyam, S. Prabha, V. Labhasetwar, Residual polyvinyl alcohol associated with poly (D,L-lactide-co-glycolide) nanoparticles affects their physical properties and cellular uptake, J Control Release, 82 (2002) 105-114.
[24] S. Prabha, W.Z. Zhou, J. Panyam, V. Labhasetwar, Size-dependency of nanoparticle-mediated gene transfection: studies with fractionated nanoparticles, Int J Pharm, 244 (2002) 105-115.
[25] A. Singhal, V.B. Morris, V. Labhasetwar, A. Ghorpade, Nanoparticle-mediated catalase delivery protects human neurons from oxidative stress, Cell Death Dis, 4 (2013) e903.
[26] T. Estey, J. Kang, S.P. Schwendeman, J.F. Carpenter, BSA degradation under acidic conditions: a model for protein instability during release from PLGA delivery systems, J Pharm Sci, 95 (2006) 1626-1639.
[27] W. Kuhlbrandt, Structure and function of mitochondrial membrane protein complexes, BMC Biol, 13 (2015) 89.
[28] D.B. Zorov, M. Juhaszova, S.J. Sollott, Mitochondrial reactive oxygen species (ROS) and ROS-induced ROS release, Physiol Rev, 94 (2014) 909-950.
[29] B.A. Citron, P.M. Arnold, C. Sebastian, F. Qin, S. Malladi, S. Ameenuddin, M.E. Landis, B.W. Festoff, Rapid upregulation of caspase-3 in rat spinal cord after injury: mRNA, protein, and cellular localization correlates with apoptotic cell death, Exp Neurol, 166 (2000) 213-226.
[30] M. Picard, Mitochondrial synapses: intracellular communication and signal integration, Trends Neurosci, 38 (2015) 468-474.
[31] K. Richetin, M. Moulis, A. Millet, M.S. Arrazola, T. Andraini, J. Hua, N. Davezac, L. Roybon, P. Belenguer, M.C. Miquel, C. Rampon, Amplifying mitochondrial function rescues adult neurogenesis in a mouse model of Alzheimer's disease, Neurobiol Dis, 102 (2017) 113-124.
[32] M. Petro, H. Jaffer, J. Yang, S. Kabu, V.B. Morris, V. Labhasetwar, Tissue plasminogen activator followed by antioxidant-loaded nanoparticle delivery promotes activation/mobilization of progenitor cells in infarcted rat brain, Biomaterials, 81 (2016) 169-180.
[33] J.W. Francis, J. Ren, L. Warren, R.H. Brown, S.P. Finklestein, Postischemic infusion of Cu/Zn superoxide dismutase or SOD: Tet451 reduces cerebral infarction following focal ischemia/reperfusion in rats, Exp Nerol, 146 (1997) 435-443.
[34] M.A. Anderson, T.M. O'Shea, J.E. Burda, Y. Ao, S.L. Barlatey, A.M. Bernstein, J.H. Kim, N.D. James, A. Rogers, B. Kato, A.L. Wollenberg, R. Kawaguchi, G. Coppola, C. Wang, T.J.

Deming, Z. He, G. Courtine, M.V. Sofroniew, Required growth facilitators propel axon regeneration across complete spinal cord injury., Nature, 561 (2018) 396-400.
[35] H. Chikuda, H. Yasunaga, K. Takeshita, H. Horiguchi, H. Kawaguchi, K. Ohe, K. Fushimi, S. Tanaka, Mortality and morbidity after high-dose methylprednisolone treatment in patients with acute cervical spinal cord injury: a propensity-matched analysis using a nationwide administrative database, Emerg Med J, 31 (2014) 201-206.
[36] G.Y. Xu, M.G. Hughes, Z. Ye, C.E. Hulsebosch, D.J. McAdoo, Concentrations of glutamate released following spinal cord injury kill oligodendrocytes in the spinal cord, Exp Neurol, 187 (2004) 329-336.
[37] F.J. Carvajal, H.A. Mattison, W. Cerpa, Role of NMDA Receptor-Mediated Glutamatergic Signaling in Chronic and Acute Neuropathologies, Neural Plast, 2016 (2016) 2701526.
[38] J.E. Springer, R.D. Azbill, P.E. Knapp, Activation of the caspase-3 apoptotic cascade in traumatic spinal cord injury, Nat Med, 5 (1999) 943-946.
[39] M. Sajic, K.K. Ida, R. Canning, N.A. Gregson, M.R. Duchen, K.J. Smith, Mitochondrial damage and "plugging" of transport selectively in myelinated small-diameter axons are major early events in peripheral neuroinflammation, J Neuroinflammation, 15 (2018) 61.
[40] X. Kong, J. Gao, Macrophage polarization: a key event in the secondary phase of acute spinal cord injury, J Cell Mol Med, 21 (2017) 941-954.

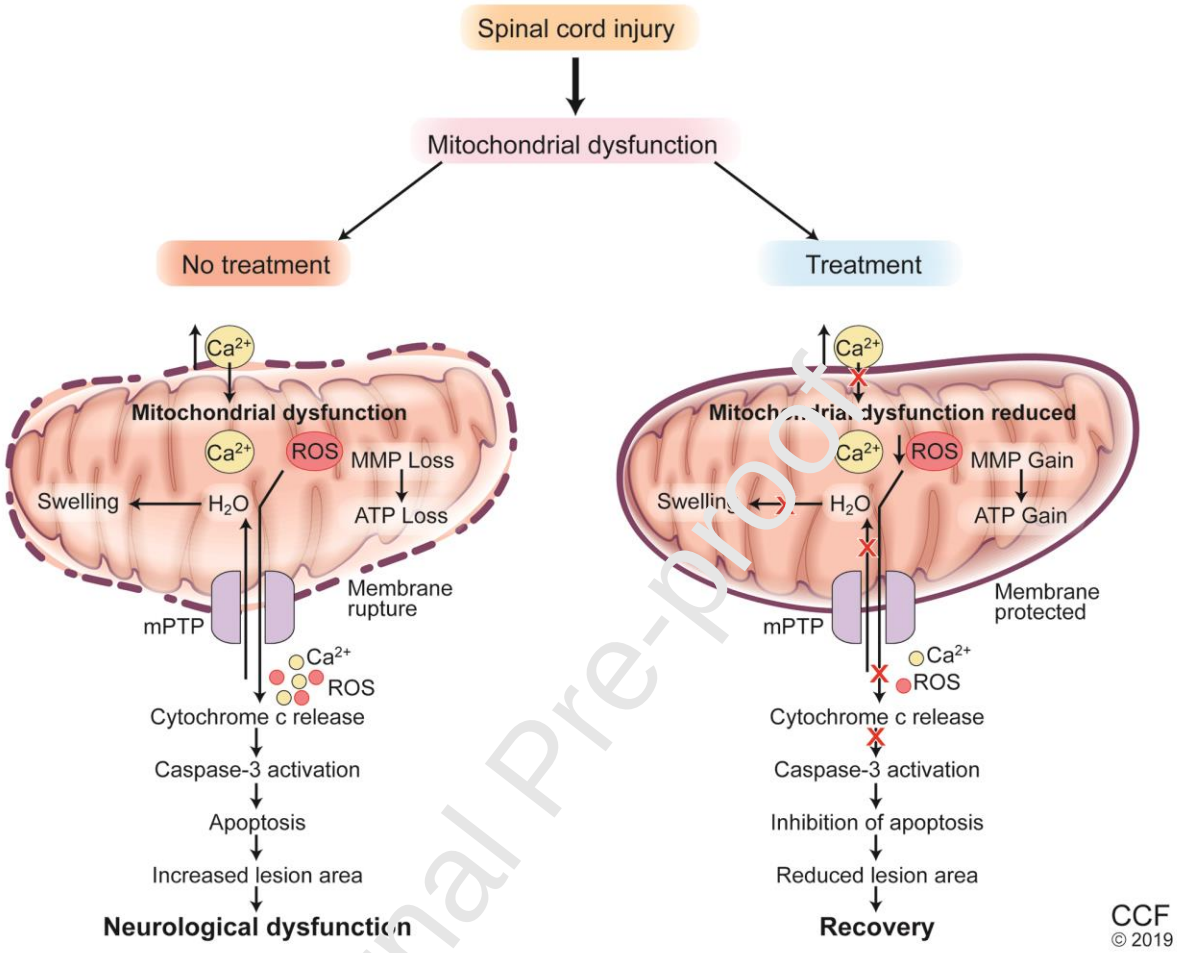

Graphical abstract

Highlights

- Spinal cord injury causes mitochondrial dysfunction
- Dysfunctional mitochondria lead to progression of secondary injury
- Nanoparticles with antioxidant enzymes protected spinal cord from secondary injury